Structure-Based Design of Peptides against G3BP with Cytotoxicity on Tumor Cells

Wei Cui,[†] Zhuo Wei,[†] Quan Chen,[†] Yuanhua Cheng,[||] Lingling Geng,[§] Jian Zhang,[§] Jianhua Chen,*[,§] Tingjun Hou,*[,‡] and Mingjuan Ji*[,†]

Department of Chemistry, Graduate University of Chinese Academy of Sciences, Beijing 100049, People's Republic of China, Functional Nano and Soft Materials Laboratory (FUNSOM) and Jiangsu Key Laboratory for Carbon-Based Functional Materials and Devices, Soochow University, Suzhou, Jiangsu 215123, People's Republic of China, Wuhan KatyGen Pharmaceuticals, Inc., Hubei Informatical Industry Building, Wujia Bay, Wuhan 430074, People's Republic of China, and, Department of Chemistry, Tsinghua University, Beijing 100084, People's Republic of China

Received October 20, 2009

Herein, we report a successful application of molecular modeling techniques to design two novel peptides with cytotoxicity on tumor cells. First, the interactions between the nuclear transport factor 2 (NTF2)-like domain of G3BP and the SH3 domain of RasGAP were studied by a well-designed protocol, which combines homology modeling, protein/protein docking, molecular dynamics simulations, molecular mechanics/generalized born surface area (MM/GBSA) free energy calculations, and MM/GBSA free energy decomposition analysis together. Then, based on the theoretical predictions, two novel peptides were designed and synthesized for biological assays, and they showed an obvious sensitizing effect on *cis*-platin. Furthermore, the deigned peptides had no significant effects on normal cells, while *cis*-platin did. Our results demonstrate that it is feasible to use the peptides to enhance the efficacy of clinical drugs and to kill cancer cells selectively. We believe that our work should be very useful for finding new therapies for cancers.

1. INTRODUCTION

Tumors are lesions formed by an abnormal growth of cells, and all tumors share the ability to proliferate without control. The Ras signaling pathway plays a pivotal role in relaying numerous regulatory networks that control cell proliferation, differentiation, and apoptosis. Mutation or mis-expression of Ras is one of the most frequent phenomena in human cancers.[1] So it is reasonable to deduce that the Ras signaling pathway is a component in the oncogenic cell signaling network. Meanwhile, the Ras−GTPase activating protein (RasGAP) has been identified as the main negative regulator of Ras.[2] RasGAP is an unconventional caspase substrate, and it can induce both anti- and pro-apoptotic signals, depending on the extent of its cleavage by caspases. At low levels of caspase activity, RasGAP is cleaved at position 455, generating N- and C-terminal fragments (fragment N and fragment C, respectively). Fragment N appears to be a general blocker of apoptosis downstream of caspase activation because it inhibits caspase9-induced cell death. At higher levels of caspase activity, fragment N is cleaved at position 157. This latter cleavage event generates two fragments, fragment N1 and fragment N2 and potently sensitizes cells toward apoptosis. The Ras-GTPase activating protein SH3 domain binding protein (G3BP), which can recognize the SH3 domain of RasGAP, overexpresses in many human tumors dramatically.[3] Several studies have shown that the RasGAP SH3 domain is important for cytoskeletal reorganization, for cell adhesion, and for induction of gene expression in a Ras-dependent manner. David Michod found that a peptide segment located from 317 to 326 in the SH3 domain of fragment N2 of RasGAP can form direct interactions with the NTF2-like domain of G3BP, which favors the apoptosis of tumor cells in response to various genotoxins.[4] A monoclonal antibody directed against the residues located from 22 to 34 of the NTF2-like domain of G3BP is specific for the G3BP-related tumor therapy.[5] Therefore, it is significant to simulate the interactions between the SH3 domain of RasGAP and the NTF2-like domain of G3BP and to design a novel peptide with cytotoxicity of tumor cells.

2. MATERIAL AND METHOD

2.1. Building the Structure Model of G3BP−RasGAP Complex. In order to simulate the interactions between the NTF2-like domain of G3BP and the SH3 domain of RasGAP (PDB entry: 2j05[6]), a homologous structure of the NTF2-like domain of G3BP (residue 3−154) was built by Modeler,[7] and the structures of NTF2 (PDB entries: 1gy5[8] and 1gy6[8]), which have the highest sequence similarities with the NTF2-like domain of G3BP from the ModBase search,[9] were selected as the templates. Sequence alignment was conducted using the CLUSTAL X 1.83 program,[10] and the default parameters were applied. Following alignment, the backbone coordinates of the residues in the NTF2-like domain of G3BP were generated using the Modeler program.[7] The homology model was then aligned to the two monomers of the template dimers to obtain the monomer homology model.

* Corresponding authors. Mingjuan Ji: E-mail: jmj@gucas.ac.cn. Telephone: +8610 88256326. Fax: +8610 88256093. Tingjun Hou: E-mail: tingjunhou@hotmail.com. Telephone: +86512 65882039. Jianhua Chen: E-mail: chenjianhua@katygenpharma.com. Telephone: +8627 87690686. Fax: +8627 87690243.

[†] Graduate University of Chinese Academy of Sciences.

[‡] Soochow University.

[§] Wuhan KatyGen Pharmaceuticals, Inc.

[||] Tsinghua University.

10.1021/ci900404p
Published on Web 02/24/2010

Molecular mechenics optimization and molecular dynamics (MD) simulations were carried out in Amber10[11] for the model of the NTF2-like domain of G3BP to get an equilibrated and reasonable structure. In the following energy minimization and MD simulations, AMBER03 (parm03) force field[12] was applied. To neutralize the charge of the systems, Na^+ ions were placed with the strongest negative Columbic potentials around the NTF2-like domain, and then the whole system was immersed in a rectangular truncated octahedron of TIP3P water molecules.[13] The water box extended 12 Å away from any solute atoms. The structure was minimized in three steps. First, all nonsolute atoms were fixed, and the water molecules were optimized (2000 cycles of both steepest descent and conjugate gradient minimizations). Second, all backbone atoms were fixed, while the side-chain atoms and the solvent were optimized (2500 cycles of both steepest descent and conjugate gradient minimizations). Finally, the whole system was optimized (2500 cycles of both steepest descent and conjugate gradient minimizations) without any constrain. After minimization, the system was heated gradually in the canonical ensemble from 0 to 310 K over 60 ps. Then an 8 ns MD simulation was performed under a constant temperature of 310 K by the weak-coupling algorithm. During the MD simulations, SHAKE[14] was used to fix all bonds involving hydrogen atoms, and the time step was set to 2 fs. Particle mesh Ewald (PME)[15] was employed to deal with the long-range electrostatic interactions. During the sampling process, coordinates were saved every 0.2 ps. The snapshot with the lowest potential energy was selected and optimized by a 2500 steps energy minimization.

The NTF2-like domain of G3BP was then docked to the SH3 domain of RasGAP using the RosettaDock 1.0 package.[16] The performance of the RosettaDock algorithm has been successfully tested in several rounds of CAPRI.[17,18] If a protein exhibits low flexibility and some helpful biological information is available, the result of RosettaDock is more credible.[19] The docking study was conducted in the following three stages: First, the global docking was performed to produce the low-resolution binding model using 300 times independent Monte Carlo searches. Second, the output structures were clustered using the kcluster program in the multiscale modeling tools for structural biology (MMTSB) tools set.[20] In each cluster, the structure with the lowest energy score was selected as the initial structure for the following perturbation searches. The normal, parallel, and rotational perturbations were set to 1 and 3 Å and 3°, respectively, and each perturbation docking study was repeated 300 times to produce the complex structure. Finally, the output structures were clustered again, and three clusters were generated. The best structure in each cluster with the most population was selected as the final docking complex to run the MD simulations.

2.2. Molecular Dynamics Simulations of the Complexes. Three independent MD simulations were carried out for three different models of complexes produced by RosettaDock. The complexes were immersed in the rectangular truncated octahedron filled with 12 Å TIP3P water molecules and neutralized by 11 Na^+ ions. For each system, all nonsolute atoms were fixed, and the water molecules were optimized first. Then, all backbone atoms were fixed, and the side chains were optimized. Finally, the whole system was optimized without any constrain. After the minimization, the systems were gradually heated in the canonical ensemble from 0 to 310 K over 60 ps, and then 5 ns MD simulation was performed under a constant temperature of 310 K. SHAKE was used, and the time step was set to 2 fs. PME was employed to deal with the long-range electrostatic interactions. During the sampling process, coordinates were saved every 0.2 ps.

2.3. Binding Free Energy Calculation. A major goal of molecular simulation in structure-based drug design is to predict the accurate binding affinities. The most time-consuming and rigorous approaches for evaluating binding affinities are the free energy perturbation (FEP) and thermodynamic integration (TI) methods. However, FEP and TI are very time consuming and can only be applied to estimate the relative binding free energy between two molecules with tiny difference. Recently, two interesting approaches named linear interaction energy (LIE) approximation and molecular mechanics/generalized born solvent area (MM/GBSA or MM/PBSA), based on MD sampling, have drawn much more attention.[21−32] Compared with LIE, MM/GBSA (MM/PBSA) does not need a fitting process to obtain the prediction model. Here, to determine the most stable RasGAP−G3BP complex given by molecular docking, the relative binding free energy ΔG_{bind} was evaluated by using the MM/GBSA technique by eq 1:[25,26]

$$\begin{aligned}\Delta G_{bind} &= G_{complex} - G_{protein} - G_{ligand} \\ &= \Delta E_{MM} + \Delta G_{GB} + \Delta G_{SA} - T\Delta S \\ &= \Delta E_{vdW} + \Delta E_{ele} + \Delta G_{GB} + \Delta G_{SA} - T\Delta S\end{aligned} \quad (1)$$

where ΔE_{MM} is the gas-phase interaction energy between protein and ligand, including the electrostatic (ΔE_{ele}) and the van der Waals energies (ΔE_{vdW}). Then, ΔG_{GB} and ΔG_{SA} are the relative polar and nonpolar components of the desolvation free energy, respectively, and $-T\Delta S$ is the change of conformational entropy upon ligand binding.

The polar solvation free energy was calculated by the generalized born (GB) model developed by Tsui and Case.[33] In the GB calculations, the solvent and the solute dielectric constants were set to 80 and 4, respectively. The nonpolar solvation term was estimated from the solvent accessible surface area (SASA). The normal-mode analysis was performed to estimate the conformational entropy change upon ligand binding ($-T\Delta S$) using the nmode program in AMBER10. Due to the high computational demand, 80 snapshots evenly extracted from 1 to 5 ns were used to estimate the binding entropy. For the other energy terms, 4000 snapshots evenly extracted from the MD trajectory of each complex structure from 1 to 5 ns were used.

2.4. Free Energy Decomposition Analysis and Peptide Design. The model B (Figure 1) with the strongest predicted binding affinity (Table 1) was selected to run the MM/GBSA free energy decomposition analysis using the mm_pbsa program in AMBER10.[34−38] The essential idea of energy decomposition was to decompose the energy contribution of each residue from the association of the receptor with the ligand into four parts: van der Waals (ΔG_{vdW}), electrostatic (ΔG_{ele}), polar part, and nonpolar of solvation ($\Delta G_{solvation}$) energies. The polar part of solvation free energy was calculated with the GB approximation model developed by Tsui,[33] and the nonpolar solvation contribution

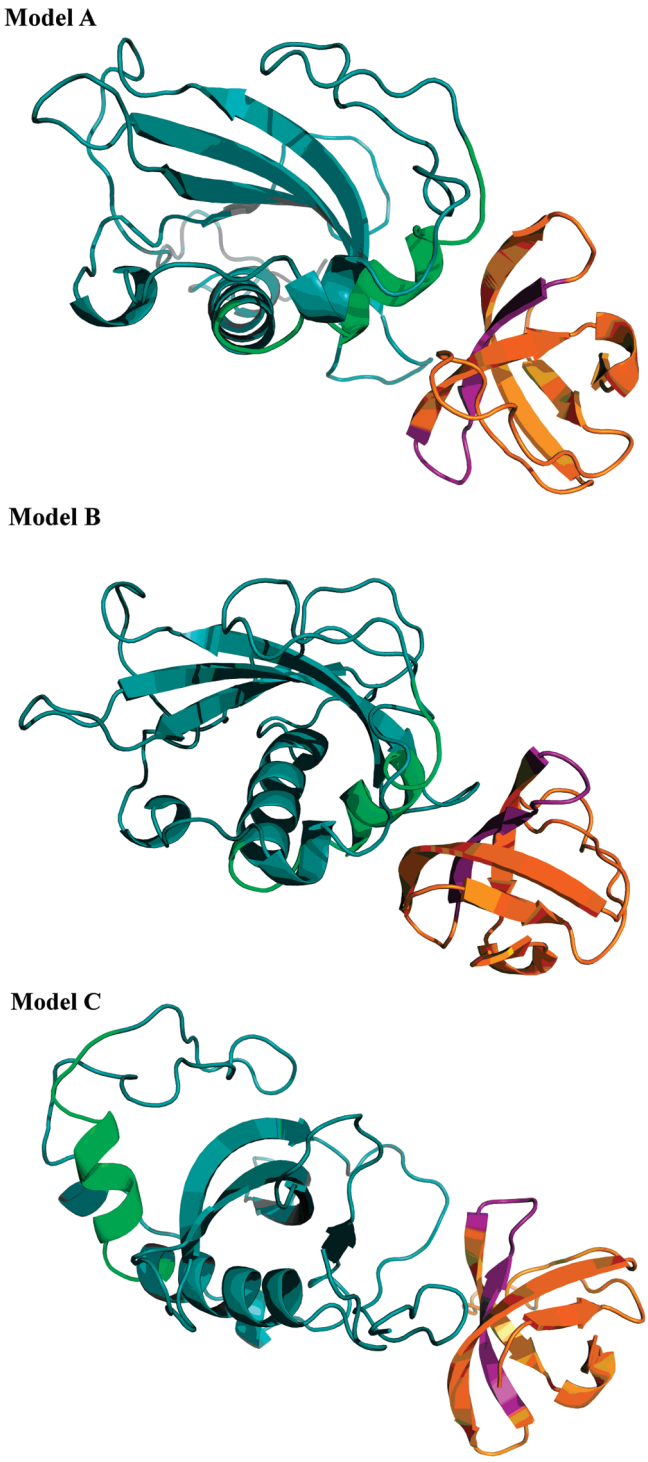

Figure 1. Three models of the NTF2-like domain of G3BP complexed with the SH3 domain of RasGAP predicted by RosettaDock. RasGAP is colored in orange, and G3BP is colored in cyan. Residues in purple are RasGAP317−326, and residues in green are G3BP22−34. The figures were generated by PyMOL (version 1.1b3).[41]

term was estimated from the surface area with the Laboratoire de Chimie des Polymres Organiques (LCPO) model.[39] Additionally all the energy terms were decomposed into backbone and side-chain contributions. The residue−residue interaction spectra given by the MM/GBSA free energy decomposition analysis may guide us to determine the key residues of the RasGAP/G3BP binding and to design more potent peptides. For energy decomposition analysis, 4000

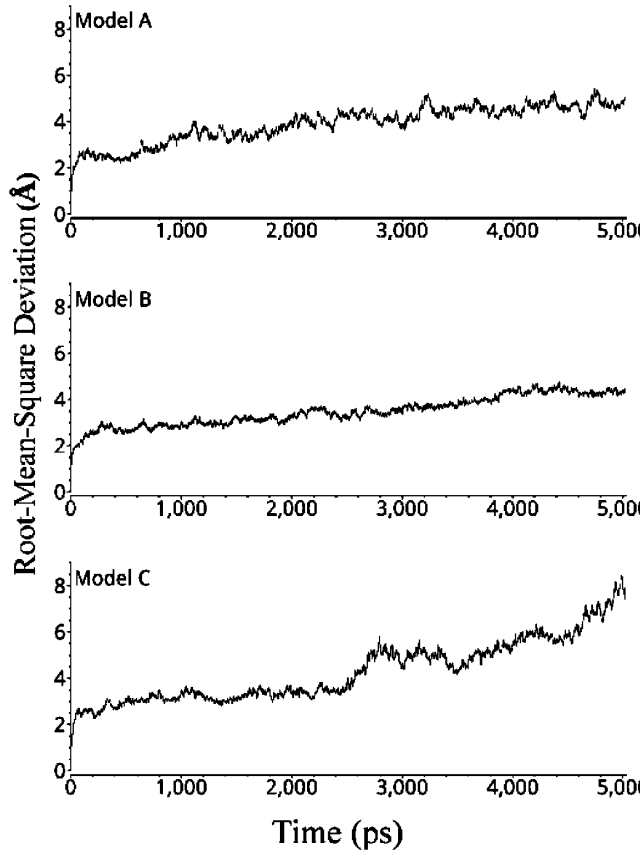

Figure 2. Root-mean-square displacement (rmsd) with respect to the first snapshot as a function of time for three models.

snapshots evenly extracted from the MD trajectory of each complex structure from 1 to 5 ns were used.

All the key residues for the RasGAP/G3BP binding were selected to design the peptide that can favor the apoptosis of tumor cells. The binding model of the novel tumor therapy peptide and the NTF-2 like domain of G3BP was built using the same strategy that we discussed above. The MD simulations were then conducted for the complex.

2.5. Peptide Synthesis and Biological Assays. The biological assays were conducted for three peptides. The sequences of the peptides are shown in Table 2. T001, RasGAP317−326, reported by Michod and co-workers, shows obvious apoptosis of tumor cells,[4] which was synthesized as the positive control peptide. P109, RasGAP301−326, is the β-sheet which was designed as the binding peptide of the NTF-2 like domain of G3BP based on the above free energy decomposition analysis. P110, RasGAP301−316, is also included for biological assay for the purpose of comparison with T001 and P109. The synthesized peptides were fused to the TAT cell permeation sequence.[40]

The peptides were synthesized by Gill Biochemical Co., Ltd., in Shanghai via the Fmoc protected amino acid solid-phase synthesis method. The unsophisticated peptides were purified using a BWAIC LC98-I high-performance liquid chromatography (HPLC) instrument with an Aglient ZORBAX 300SB-C18 reversed phase column. Peptides were eluted with a linear gradient of water, H_2O, and acetonitrile, ACN, (both having 0.1% TFA) at a flow rate of 1 mL/min (Table 3). The separation was monitored at 220 nm using UV detection. Then peptides were subjected to mass

Table 1. The Binding Free Energies between The NTF2-like Domain of G3BP and the SH3 Domain of RasGAP for the Three Final Complexes Calculated by MM/GBSA (kcal/mol)

	model A	model B	model C
ΔG_{TOT}	-48.7 ± 2.4	-61.5 ± 3.7	-34.8 ± 10.7
ΔG_{ele}	-17.0 ± 7.6	33.0 ± 4.2	24.2 ± 27.4
ΔG_{vdW}	-46.3 ± 2.1	-62.1 ± 3.5	-37.1 ± 7.8
ΔG_{SA}	8.2 ± 0.2	-11.0 ± 0.5	6.9 ± 1.6
ΔG_{GB}	22.9 ± 7.0	-21.5 ± 4.3	-15.0 ± 25.2
$T\Delta S$	-39.6 ± 7.5	-37.5 ± 8.0	-33.2 ± 7.4

Table 2. The Sequences and Biological Assays for Three Peptides and for *cis*-Platin

name	sequence	IC_{50} (μM)
T001	WMWVTNLRTD	–
P109	FLKGDMFIVHNELEDGWMWVTNLRTD	11.75
P110	FLKGDMFIVHNELEDG	27.64
cis-platin combined with P109	FLKGDMFIVHNELEDGWMWVTNLRTD	2.27
cis-platin	–	9.48

Table 3. Gradient for Peptide Purification

time	percent[a]	percent[b]
0	100	0
30	10	90
33	10	90
34	100	0

[a] Solvent: 100% H_2O + 0.1% TFA. [b] Solvent: 100% ACN + 0.1% TFA.

spectrometric (MS) analysis. The solvents for gradient elution HPLC are: solvent A, H_2O 99.9%, TFA 0.1% and solvent B, ACN 99.9%, TFA 0.1%.

Peptides were dissolved in deionized H_2O at a final concentration of 1 mM and stored at −20 °C until further use. As comparison, the biological assay was also conducted for *cis*-platin, a classical drug used to treat various types of cancers. *Cis*-platin was dissolved in a phosphate-buffered saline solution at a final concentration of 3.3 mM, stored at −20 °C.

Human cervical cancer Hela cells and human myoblasts were purchased from the Preservation Center of Wuhan University. Hela cells were maintained in a minimum essential medium (GIBCO; cat no. 41500−034), containing 10% fetal calf serum at 37 °C and 5% CO2. Myoblasts were maintained in RPMI 1640 (GIBCO; cat no. 31800−022), containing 10% fetal calf serum at 37 °C and 5% CO2.

Genotoxin treatment was performed in 96-well plates. The cells were digested with 0.25% trypsin into a single cell suspension, adjusting the cell density of 2×10^4/mL. Then, 200 μL of cells were cultured in 96 wells. When the cell density in 96 wells reached 70%−80%, 24 h later, the cells were incubated for 20 h with the indicated concentrations of *cis*-platin and peptide. Then, 180 μL of MTT (0.5 mg/mL) was added to each well. The culture medium was cleared 4 h later. After adding 150 μL of DMSO to each well, the plate was concussed for 10 min, making the purple crystalline fully dissolved. The effect was determined by a microplate reader at 570 nm absorbance.

3. RESULTS AND DISCUSSIONS

3.1. Predictions of the G3BP−RasGAP complex by protein/protein docking. Three different possible binding models were identified by protein/protein docking studies of RosettaDock (shown in Figure 1). In model A, the distance between residues RasGAP317−326 and G3BP22−34 is 10.37 Å, and those residues are interacted directly. In model B, the same distance is 16.03 Å, which shows the residue RasGAP317−326 does not form a direct interaction with G3BP22−34, while G3BP22−34 is still in the binding interface of these two proteins. In model C, the distance is 32.66 Å, showing the residue RasGAP317−326 is far from the residue G3BP22−34.

3.2. MD Simulation and MM/GBSA Free Energy Calculation. Figure 2 shows the evolutions of the root-mean-square displacement (rmsd) values for the three complexes given by the docking studies. The fluctuations of rmsd show that model B is stable after ∼800 ps, while the other two systems even become unstable after 2.5 ns. The predicted binding free energies between the NTF2-like domain of G3BP and the SH3 domain of RasGAP by MM/GBSA are shown in Table 1 (see also Figure 3). According to the predicted binding free energies, model B is much more stable than the others. That is to say, the residues RasGAP317−326 and G3BP22−34 are located in the binding interface of RasGAP and G3BP, while they do not form direct interactions.

3.3. MM/GBSA Free Energy Decomposition Analysis and Peptide Design. In order to gain a clear picture about the contribution of each residue of the SH3 domain of RasGAP and the NTF2-like domain of G3BP to binding, the total binding free energy of model B was decomposed into residue−residue interaction pairs, using the MM/GBSA free energy decomposition analysis. The residue−residue interaction spectra in Figure 4 shows that the residues 305−326 in RasGAP are the most important contributors for the interactions between the NTF2-like domain of G3BP and the SH3 domain of RasGAP.

According to Table 4, the residues Ile308, Val309, His310, Asn311, and Thr321 of the SH3 domain of RasGAP form strong interactions with the residues Asp28, Met29, His31, and Arg32 of the NTF2-like domain, and those residues are the epitope of the monoclonal antibody against the NTF2-like domain with the G3BP-related tumor therapy effect.[4] Moreover, the residues His310, Asn311, Leu313, and Trp319 of the SH3 domain also form effective interactions with the residues Glu117, Gly118, Tyr125, Val126, and His127 of the NTF2-like domain.

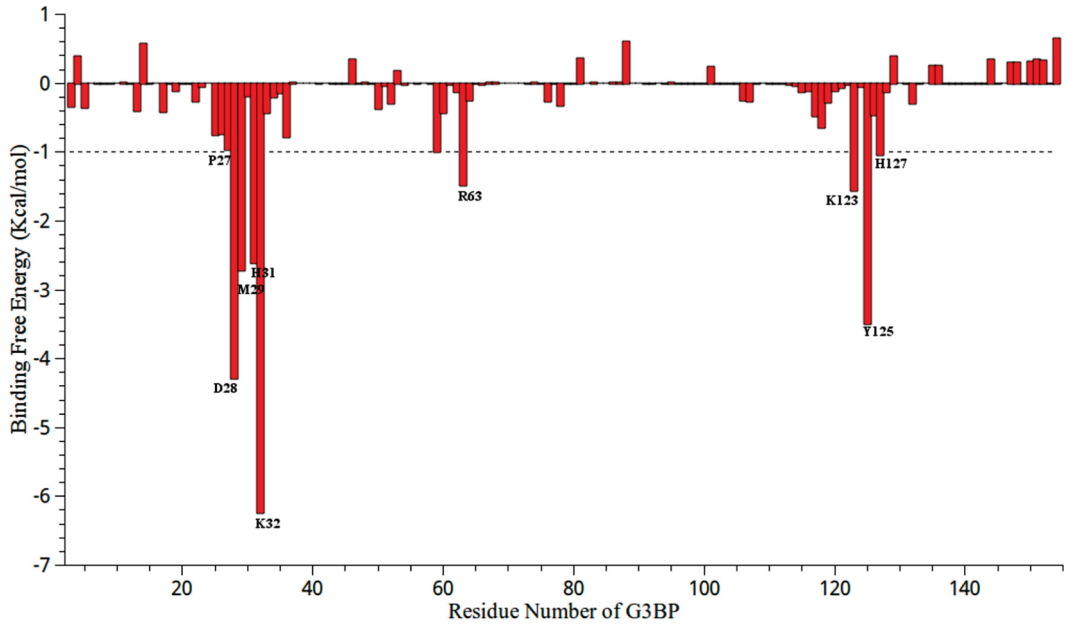

(a)

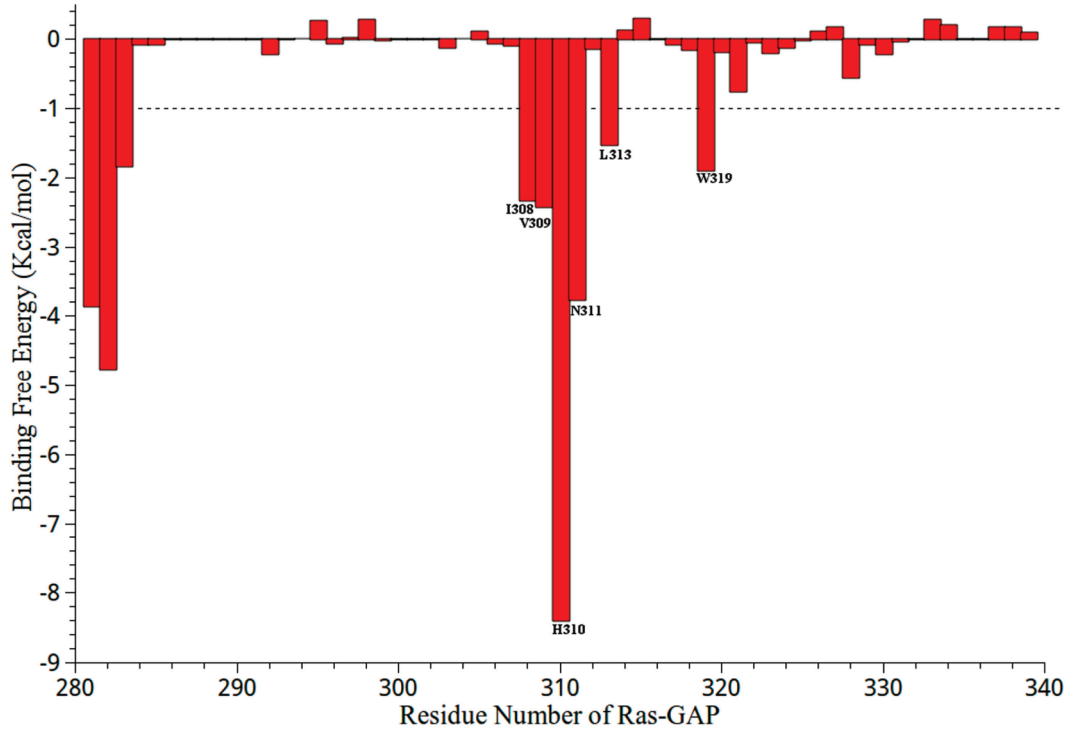

(b)

Figure 3. The contributions of each residue in (a) the NTF2-like domain of G3BP and (b) the SH3 domain of RasGAP calculated by the MM/GBSA free energy decomposition analysis. The important residues were labeled.

According to the results of the MM/GBSA free energy decomposition analysis (Figure 5), RasGAP307−321 are the key residues for the binding between RasGAP and G3BP, and the structure analysis shows that those key residues belong to a β-sheet. Considering the energy contribution of the key residues and the structural independence of the secondary structures in the SH3 domain of RasGAP, a peptide segment with a β-sheet located from the residues 301−326 was picked out to build the binding model again (Figure 4). MD simulations were then conducted for the peptide complexed with the NTF2-like domain of G3BP. Root-mean-square fluctuations (rmsf) of the backbone atoms of the peptide shows that the average rmsf values of the peptide from 301−326 is about 4.87 Å, while the value of the same position in the whole SH3 domain is 4.23 Å. The similarity of the rmsf values implies that the peptide can also form stable complex with the NF2-like domain.

3.4. Biological Assays. According to the results of HPLC and MS, the retention time (R_t) of peptides T001, P109 and P110 (Table 2) are 17.36, 19.442, and 17.687 min, resec-

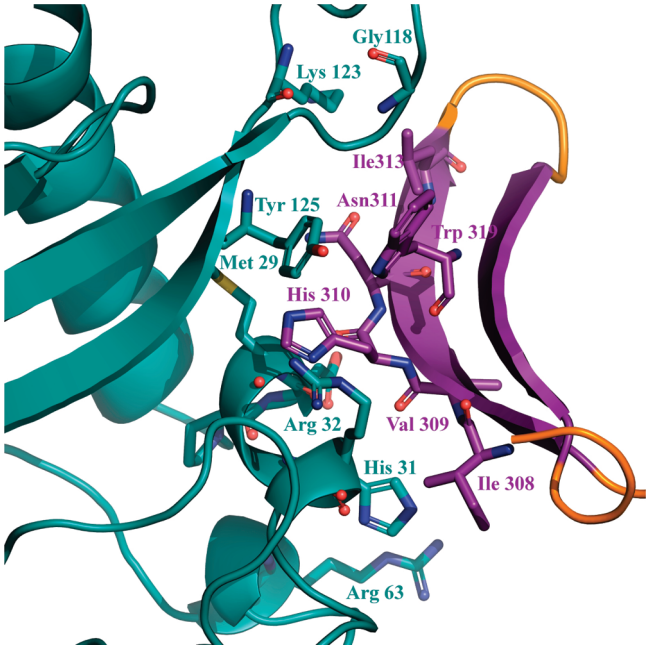

Figure 4. The interactions between the peptide P109 and the NTF2-like domain of G3BP. P109 is colored in purple and orange, and G3BP is colored in cyan. All the important residues are shown in a stick form. The figure was generated by PyMOL (version 1.1b3).[41]

tively, and the molecular weight of the peptides is 2813.29, 3412.96, and 4660.41, respectively, which are consistent with the theoretical values.

The results of the biological assays are shown in Figure 5. In Figure 5a, combined with peptide P110, P109, or T001 at a concentration of 20 μM, *cis*-platin shows stronger biological activity than when used alone on Hela cells. The peptide P110 has the most remarkable sensitizing effect on *cis*-platin, followed by the peptide P109. The peptides P110 and P109 have a better sensitizing effect on *cis*-platin than that of T001. Furthermore, when the concentration of *cis*-platin is 0 μM, the inhibitory rates of the peptides P110 and P109 to Hela cells are still 17.6% and 17.7%, respectively, while that of the peptide T001 is only 2.5%, implying that those two peptides not only have sensitizing effects on *cis*-platin but also have distinguished inhibitions on Hela cells. Then, we tested the effects of the three peptides and the *cis*-platin on human myoblasts individually. In Figure 5b, *cis*-platin has apparent killing effects on human myoblasts, while at the same concentration the peptide P110, P109, or T001 does not kill human myoblasts. In short, three peptides have no significant effects on normal cells in low concentration.

To determine the tumor-killing capabilities of P109 and P110, we measured the IC_{50} of them, individually, and the IC_{50} of *cis*-platin combined with peptides at a concentration of 20 μM. The results are shown in Table 2. The IC_{50} values of P110 and P109 are 27.64 and 11.75 μM, respectively, which are the same order of magnitude of 9.48 μM, IC_{50} of *cis*-platin. Combined with P110 at the concentration of 20 μM, the IC_{50} value of *cis*-platin is 2.27 μM, which is over three times lower than that of *cis*-platin. These data ensure that P109 and P110 have obvious inhibitions on Hela cells, and P109 has a sensitizing effect on *cis*-platin.

4. CONCLUSIONS

In the current work, the interactions between the NTF2-like domain of G3BP and the SH3 domain of RasGAP were successfully predicted by molecular modeling techniques. Based on the predicted models, two peptides (P109 and P110) were designed and synthesized, and their biological activities were confirmed by experiments.

Our experimental results still show that it is feasible to use P109 or P110 to enhance the efficacy of clinically used drugs, for example, *cis*-platin, and to kill cancer cells selectively. Moreover, according to the results of molecular modeling, the reason why P110 and P109 lead to the

Table 4. The Contribution of the Key Residues in RasGAP to the Interactions Between RasGAP and G3BP (kcal/mol)

RasGAP	G3BP	ΔG_{total}	ΔG_{vdW}	ΔG_{ele}	ΔG_{gas}	ΔG_{GB}	ΔG_{SA}	ΔG_{GBSA}
Ile308		−2.2	−2.1	−0.4	−2.4	0.6	−0.4	0.2
Ile308	His31	−0.1	−0.1	−0.0	−0.2	0.0	−0.0	−0.0
Ile308	Arg32	−2.1	−1.1	−0.2	−1.3	0.2	−1.0	−0.8
Val309		−2.4	−2.5	0.0	−2.5	0.3	−0.2	0.1
Val309	Asp28	−1.9	−1.1	0.1	−1.0	0.3	−0.6	−0.9
His310		−8.4	−8.1	−1.5	−9.6	2.3	−1.1	1.2
His310	Asp28	−1.6	−1.1	0.1	−1.0	−0.1	−0.5	−0.6
His310	Met29	−2.0	−1.2	−0.1	−1.3	0.1	−0.8	−0.7
His310	Arg32	−3.6	−1.8	−0.4	−2.3	−0.2	−1.6	−1.3
His310	Tyr125	−2.2	−1.2	−0.4	−1.6	0.2	−0.9	−0.7
His310	Val126	−0.6	−0.4	−0.2	−0.5	0.1	−0.2	−0.1
His310	His127	−1.9	−1.0	−0.3	−1.3	0.2	−0.8	−0.6
Asn311		−3.8	−3.4	−1.1	−4.6	1.3	−0.6	0.8
Asn311	Asp28	−0.7	−0.4	0.0	−0.4	−0.1	−0.2	−0.3
Asn311	Met29	−1.2	−0.6	−0.1	−0.7	0.0	−0.6	−0.6
Asn311	Glu117	−1.4	−0.3	−1.0	−1.3	0.5	−0.5	−0.1
Asn311	Tyr125	−2.3	−1.3	−0.1	−1.4	0.1	−0.9	−0.9
Leu313		−1.6	−1.4	−0.3	−1.7	0.4	−0.2	0.1
Leu313	Glu117	−1.9	−1.0	−0.8	−1.7	0.6	−0.9	−0.2
Trp319		−1.5	−1.5	0.5	−1.0	−0.3	−0.2	−0.5
Trp319	Glu117	−0.2	−0.1	0.1	−0.0	−0.1	−0.0	−0.1
Trp319	Gly118	−1.1	−0.6	0.1	−0.6	−0.0	−0.5	−0.6
Trp319	Tyr125	−0.8	−0.6	−0.2	−0.8	0.2	−0.1	0.0
Thr321		−1.2	−0.4	−0.2	−0.7	−0.0	−0.5	−0.5
Thr321	Arg32	−0.7	−0.1	−0.1	0.2	−0.0	−0.4	0.6

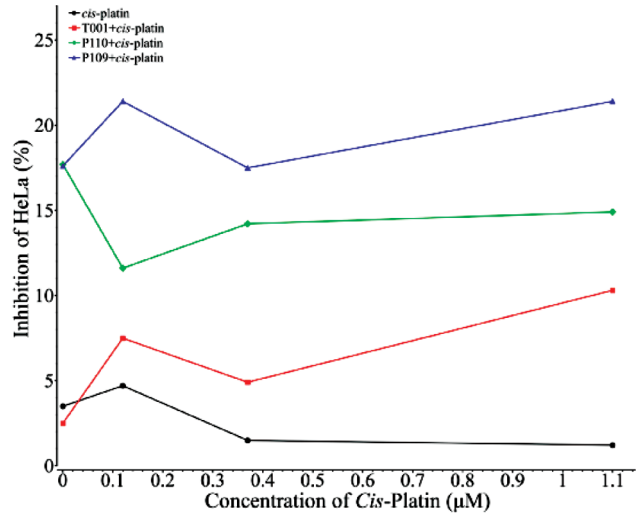

Figure 5. Biological assays of (a) *cis*-platin combined with peptide P110, P109, or T001 at a concentration of 20 μM on Hela cells and (b) peptide P110, P109, T001 and *cis*-platin on myoblasts.

apoptosis of tumor cells can be explained by the competitive interruption of the interactions between RasGAP and G3BP. Now, based on the predicted complex, a virtual mutagenesis study is on the way. We expect that we can design peptides with higher affinities by mutating the key residues in P109. In parallel, two-dimension NMR and crystal structural studies of the complex formed by RasGAP and G3BP or of that formed by P109 and G3BP should be very helpful.

ACKNOWLEDGMENT

The project was supported by the National Science and Technology Major Special Project of China (No. 2009ZX09501-011) and the Natural Science Foundation of China (No. 20973121).

REFERENCES AND NOTES

(1) Bos, J. L. Ras Oncogenes in Human Cancer - a Review. *Cancer Res.* **1989**, *49*, 4682–4689.
(2) Mccormick, F. Ras Gtpase Activating Protein - Signal Transmitter and Signal Terminator. *Cell* **1989**, *56*, 5–8.
(3) Guitard, E.; Parker, F.; Millon, R.; Abecassis, J.; Tocqué, B. G3BP is overexpressed in human tumors and promotes S phase entry. *Cancer lett.* **2001**, *162*, 213–221.
(4) Michod, D.; Yang, J. Y.; Chen, J. H.; Bonny, C.; Widmann, C. A RasGAP-derived cell permeable peptide potently enhances genotoxin-induced cytotoxicity in tumor cells. *Oncogene* **2004**, *23*, 8971–8978.
(5) Parker, F.; Kenigsberg, M.; Duchesne, M.; Barlat, I. Monoclonal Antibodies Directed against the G3BP Protein, and Uses: French, 1999.
(6) Parker, F.; Maurier, F.; Delumeau, I.; Duchesne, M.; Faucher, D.; et al. A ras-GTPase-activating protein SH3-domain-binding protein. *Mol. Cell. Biol.* **1996**, *16*, 2561–2569.
(7) Fiser, A. S.; Sali, A. MODELLER: Generation and refinement of homology-based protein structure models. *Macromol. Crystallography, Pt D* **2003**, *374*, 461+.
(8) Bayliss, R.; Leung, S. W.; Baker, R. P.; Quimby, B. B.; Corbett, A. H.; et al. Structural basis for the interaction between NTF2 and nucleoporin FxFG repeats. *EMBO J.* **2002**, *21*, 2843–2853.
(9) Pieper, U.; Eswar, N.; Braberg, H.; Madhusudhan, M.; Davis, F.; Stuart, A.; Mirkovic, N.; Rossi, A.; Marti-Renom, M.; Fiser, A.; et al. MODBASE, a database of annotated comparative protein structure models, and associated resources. *Nucleic Acids Res.* **2004**, *32*, D217.
(10) Thompson, J.; Gibson, T.; Plewniak, F.; Jeanmougin, F.; Higgins, D. The CLUSTAL_X windows interface: flexible strategies for multiple sequence alignment aided by quality analysis tools. *Nucleic Acids Res.* **1997**, *25*, 4876–4882.
(11) Case, D. A.; Cheatham, T. E.; Darden, T.; Gohlke, H.; Luo, R.; et al. The Amber biomolecular simulation programs. *J. Comput. Chem.* **2005**, *26*, 1668–1688.
(12) Duan, Y.; Wu, C.; Chowdhury, S.; Lee, M. C.; Xiong, G. M.; et al. A point-charge force field for molecular mechanics simulations of proteins based on condensed-phase quantum mechanical calculations. *J. Comput. Chem.* **2003**, *24*, 1999–2012.
(13) Jorgensen, W. L.; Chandrasekhar, J.; Madura, J. D.; Impey, R. W.; Klein, M. L. Comparison of Simple Potential Functions for Simulating Liquid Water. *J. Chem. Phys.* **1983**, *79*, 926–935.
(14) Ryckaert, J. P.; Ciccotti, G.; Berendsen, H. J. C. Numerical-Integration of Cartesian Equations of Motion of a System with Constraints - Molecular-Dynamics of N-Alkanes. *J. Chem. Phys.* **1977**, *23*, 327–341.
(15) Darden, T.; York, D.; Pedersen, L. Particle Mesh Ewald - an N.Log(N) Method for Ewald Sums in Large Systems. *J. Chem. Phys.* **1993**, *98*, 10089–10092.
(16) Gray, J. J.; Moughon, S.; Wang, C.; Schueler-Furman, O.; Kuhlman, B.; et al. Protein-protein docking with simultaneous optimization of rigid-body displacement and side-chain conformations. *J. Mol. Biol.* **2003**, *331*, 281–299.
(17) Daily, M. D.; Masica, D.; Sivasubramanian, A.; Somarouthu, S.; Gray, J. J. CAPRI rounds 3−5 reveal promising successes and future challenges for RosettaDock. *Proteins: Struct., Funct., Bioinf.* **2005**, *60*, 181–186.
(18) Gray, J. J.; Moughon, S. E.; Kortemme, T.; Schueler-Furman, O.; Misura, K. M. S.; et al. Protein-protein docking predictions for the CAPRI experiment. *Proteins: Struct., Funct., Genet.* **2003**, *52*, 118–122.
(19) Janin, J.; Henrick, K.; Moult, J.; Ten Eyck, L.; Sternberg, M. J. E.; et al. CAPRI: A Critical Assessment of PRedicted Interactions. *Proteins: Struct., Funct., Bioinf.* **2003**, *52*, 2–9.
(20) Feig, M.; Karanicolas, J.; Brooks, C. L. MMTSB Tool Set: enhanced sampling and multiscale modeling methods for applications in structural biology. *J. Mol. Graphics Modell.* **2004**, *22*, 377–395.
(21) Aqvist, J.; Medina, C.; Samuelsson, J. E. A new method for predicting binding affinity in computer-aided drug design. *Protein Eng.* **1994**, *7*, 385–391.
(22) Hou, T. J.; Guo, S. L.; Xu, X. J. Predictions of binding of a diverse set of ligands to gelatinase-A by a combination of molecular dynamics and continuum solvent models. *J. Phys. Chem. B* **2002**, *106*, 5527–5535.
(23) Bren, U.; Martinek, V.; Florian, J. Free Energy Simulations of Uncatalyzed DNA Replication Fidelity: Structure and Stability of T.G and dTTP.G Terminal DNA Mismatches Flanked by a Single Dangling Nucleotide. *J. Phys. Chem. B* **2006**, *110*, 10557–10566.
(24) Perdih, A.; Bren, U.; Solmajer, T. Binding free energy calculations of N-sulphonyl-glutamicacid inhibitors of MurD ligase. *J. Mol. Graphics Modell.* **2009**, *15*, 983–996.
(25) Wang, J. M.; Hou, T. J.; Xu, X. J. Recent advances in free energy calculations with a combination of molecular mechanics and continuum models. *Curr. Comput.-Aided Drug Des.* **2006**, *2*, 287–306.
(26) Kollman, P. A.; Massova, I.; Reyes, C.; Kuhn, B.; Huo, S. H.; et al. Calculating structures and free energies of complex molecules: Combining molecular mechanics and continuum models. *Acc. Chem. Res.* **2000**, *33*, 889–897.
(27) Kuhn, B.; Kollman, P. A. Binding of a diverse set of ligands to avidin and streptavidin: An accurate quantitative prediction of their relative affinities by a combination of molecular mechanics and continuum solvent models. *J. Med. Chem.* **2000**, *43*, 3786–3791.

(28) Wang, W.; Kollman, P. A. Computational study of protein specificity: The molecular basis of HIV-1 protease drug resistance. *Proc. Natl. Acad. Sci. U.S.A.* **2001**, *98*, 14937–14942.
(29) Hou, T. J.; Zhu, L. L.; Chen, L. R.; Xu, X. J. Mapping the binding site of a large set of quinazoline type EGF-R inhibitors using molecular field analyses and molecular docking studies. *J. Chem. Inf. Comput. Sci.* **2003**, *43*, 273–287.
(30) Lepsik, M.; Kriz, Z.; Havlas, Z. Efficiency of a second-generation HIV-1 protease inhibitor studied by molecular dynamics and absolute binding free energy calculations. *Proteins: Struct., Funct., Bioinf.* **2004**, *57*, 279–293.
(31) Hou, T. J.; Chen, K.; McLaughlin, W. A.; Lu, B. Z.; Wang, W. Computational analysis and prediction of the binding motif and protein interacting partners of the Abl SH3 domain. *PloS Comput. Biol.* **2006**, *2*, 46–55.
(32) Hou, T.; Yu, R. Molecular dynamics and free energy studies on the wild-type and double mutant HIV-1 protease complexed with amprenavir and two amprenavir-related inhibitors: Mechanism for binding and drug resistance. *J. Med. Chem.* **2007**, *50*, 1177–1188.
(33) Tsui, V.; Case, D. A. Theory and applications of the generalized Born solvation model in macromolecular Simulations. *Biopolymers* **2000**, *56*, 275–291.
(34) Hou, T. J.; Zhang, W.; Case, D. A.; Wang, W. Characterization of domain-peptide interaction interface: A case study on the amphiphysin-1 SH3 domain. *J. Mol. Biol.* **2008**, *376*, 1201–1214.
(35) Gohlke, H.; Kiel, C.; Case, D. A. Insights into protein-protein binding by binding free energy calculation and free energy decomposition for the Ras-Raf and Ras-RaIGDS complexes. *J. Mol. Biol.* **2003**, *330*, 891–913.
(36) Hou, T. J.; Xu, Z.; Zhang, W.; McLaughlin, W. A.; Case, D. A.; et al. Characterization of Domain-Peptide Interaction Interface: a generic structure-based model to decipher the binding specificity of SH3 domains. *Mol. Cell. Proteomics* **2009**, *8*, 639–649.
(37) Bren, M.; Florián, J.; Mavri, J.; Bren, U. Do all pieces make a whole? Thiele cumulants and the free energy decomposition. *Theor. Chim. Acta.* **2007**, *117*, 535–540.
(38) Bren, U.; Martinek, V.; Florián, J. Decomposition of the Solvation Free Energies of Deoxyribonucleoside Triphosphates Using the Free Energy Perturbation Method. *J. Phys. Chem. B* **2006**, *110*, 12782–12788.
(39) Weiser, J.; Shenkin, P. S.; Still, W. C. Approximate atomic surfaces from linear combinations of pairwise overlaps (LCPO). *J. Comput. Chem.* **1999**, *20*, 217–230.
(40) Michod, D.; Widmann, C. TAT-RasGAP(317−326) requires p53 and PUMA to sensitize tumor cells to genotoxins. *Mol. Cancer Res.* **2007**, *5*, 497–507.
(41) DeLano, W. L. *The PyMOL Molecular Graphics System*; DeLano Scientific: Palo Alto, CA, 2002.

CI900404P